American Mineralogist, Volume 66, pages 51-69, 1981

Metamorphic petrology, mineral equilibria, and polymetamorphism in the Augusta quadrangle, south-central Maine

JAMES M. NOVAK[1] AND M. J. HOLDAWAY

Department of Geological Sciences
Southern Methodist University, Dallas, Texas 75275

Abstract

A study of pelitic metamorphism in the western 70 percent of the Augusta quadrangle, Maine, has shown that this metamorphic terrane consists of products of a series of overlapping thermal events. Prograde isograds have been delineated on the basis of discontinuous reactions. Continuous reactions are also described, based on Fe–Mg–Mn phase relations and garnet zoning patterns.

Two approaches have been used to estimate the pressure and temperature of the lower sillimanite zone. Fe–Mg K_D's from garnet–biotite pairs were used to estimate the temperature of metamorphism. Reactions involving staurolite were also used after adjusting their experimentally determined reaction curves for variations in mineral compositions and the composition of the fluid phase. Assuming the presence of an independent fluid phase, calculations show that $X(H_2O)$ was on the order of 0.75±0.10. Results indicate that the average temperature and pressure of the lower sillimanite zone were 570±40°C, 3.8±1 kbar.

Field relations indicate that the metamorphism, both prograde and retrograde, was closely associated with the emplacement of felsic plutonic bodies. The sequence of events postulated for the Augusta area is as follows: (1) a widespread andalusite–biotite–staurolite-producing event of uncertain cause, was followed by (2) a sillimanite-producing event whose heat source was southeast of the area. This event produced widespread slight retrogressive metamorphism to the north. (3) The final metamoprhic event was also sillimanite-producing, with a heat source supplied by a group of plutons west of the Augusta quadrangle. This event caused localized intense retrogressive metamorphism along a NNE-trending zone in the western part of the Augusta quadrangle.

Introduction

A classic pattern of regional metamorphism is presented in Maine by the distribution of isograds which delineate zones of metamorphic grade ranging from sub-chlorite in the extreme northeastern part of the state to sillimanite–K feldspar in the southwest (Doyle, 1967). Important contributions to the study of metamorphism of pelitic rocks in Maine have been made by Guidotti (1963, 1970a, 1970b, 1974) in the region near Rangeley and by Osberg (1968, 1971, 1974) in the Waterville–Vassalboro area. Guidotti's studies have shown that the regional isograds are actually composite features, formed by more than one metamorphic episode. These overlapping events complicate detailed petrologic studies and make accurate estimates of pressure–temperature relations difficult.

We report the results of a moderately detailed study of metamorphism in the western 70 percent of the Augusta 15-minute quadrangle in south-central Maine (Fig. 1). Mineral assemblages in the pelitic rocks indicate that amphibolite facies conditions prevailed throughout most of the area. The results show that polymetamorphism played an important role in shaping the metamorphic history. Various reactions have been deduced, based on AFM topology changes, garnet zoning patterns, and element distribution between minerals. Reaction isograds have been drawn on the basis of these reactions. We hope that this work will help provide insights into the metamorphism in Maine through a better understanding of the types of processes which occurred in this area.

[1] Present address: Air Force Geophysics Laboratory, Hanscom A.F.B., Massachusetts 01731.

0003–004X/81/0102–0051$02.00

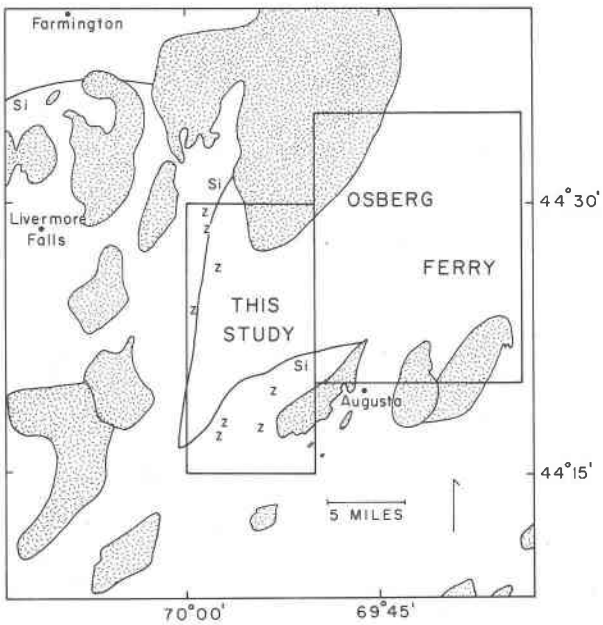

Fig. 1. Locality map of study area. Random line pattern = plutonic igneous rocks, Si = high-grade side of sillimanite isograd, Z = localities where zoisite or clinozoisite occurs in calcareous rocks. Osberg (1968) worked mainly on pelites in the northwest part of the indicated area; Ferry (1976a,b) worked mainly on calcareous rocks in the southeast part of the area. Distribution of plutonic rocks is based on Preliminary Lithologic Map of Maine (unpublished, compiled by P. H. Osberg, 1973, Maine Geological Survey).

During the summer of 1977 reconnaissance geologic mapping and more detailed specimen sampling (Fig. 2) were undertaken. The degree of outcrop and the reconnaissance nature of the mapping did not allow us to make any meaningful contribution to the stratigraphy and structure of the area (Novak, 1978).

Geologic setting

The Augusta area lies on the southeast limb of the Merrimack Synclinorium, one of the major structural features of New England. The general geology and stratigraphy of the Merrimack Synclinorium in Maine have been described by Osberg *et al.* (1968) and more recently by Pankiwskyj *et al.* (1976). An overview of the deformation, plutonism, and polymetamorphism in western Maine is given by Moench and Zartman (1976).

Our samples were collected from pelitic layers of the Silurian Waterville and Mayflower Hill Formations (Osberg, 1968; Novak, 1978). The calcareous Vassalboro Formation is locally exposed within the study area. Igneous rocks consist mainly of two plutons of biotite–muscovite–garnet-bearing quartz monzonite. Dallmeyer and Vanbreeman (1978) report Rb–Sr whole-rock isochron ages for the Hallowell Pluton at Augusta and the Togus pluton to the east of Augusta as 387±11 and 394±8 m.y. respectively. Possibly the Skowhegan pluton at the northeastern edge of the map area is of comparable age. Moench and Zartman (1976) report a Rb–Sr whole-rock age of 379±6 m.y. for the Mooselookmeguntic two-mica granite about 60 km northwest of the map area.

Petrology

In discussing the petrology of pelitic rocks, we will first summarize the petrographic characteristics of the minerals, then discuss the mineral chemistry, and finally relate the textures and mineral assemblages to the metamorphic pattern in the area. Poorly exposed

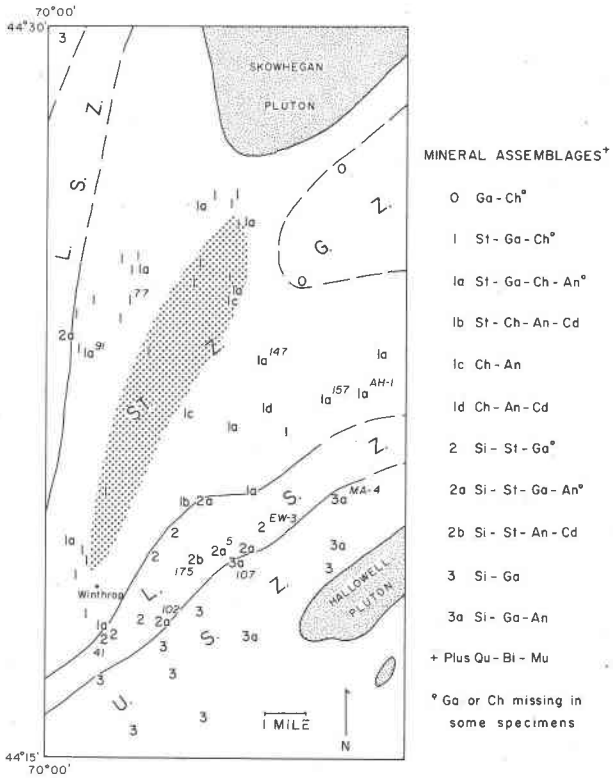

Fig. 2. Pelitic mineral assemblage and isograd map of the western 70 percent of the Augusta 15-minute quadrangle. Random line pattern = biotite–muscovite–garnet quartz monzonite, heavy stipple = zone of partially retrograded rocks, italicized numbers = localities of specimens whose minerals were analyzed. Mineral abbreviations for this and other figures: Ga = almandine-rich garnet, Ch = chlorite, St = staurolite, An = andalusite, Cd = cordierite, Si = sillimanite, Qu = quartz, Bi = biotite, Mu = muscovite. Metamorphic zones: G. Z. garnet zone, ST. Z. = staurolite zone, L. S. Z. = lower sillimanite zone, U. S. Z. = upper sillimanite zone.

rocks of the garnet zone occur in the northeastern part of the area (Fig. 2). From here, grade increases to the west and south. Around the garnet zone is a broad staurolite zone. At the western edge are rocks of the lower sillimanite zone (staurolite present). Similar grade rocks are exposed in the south-central part. In the southeastern and northwestern parts are upper sillimanite-zone rocks (without staurolite). Parallel to the western sillimanite isograd is a zone of partial retrograde metamorphism within the staurolite zone (Fig. 2).

Petrography

In all pelitic rocks brown or red-brown biotite and muscovite are dominant matrix minerals, defining schistosity as fine imperfectly oriented grains. With increasing grade some biotite takes on a slightly porphyroblastic habit with weaker preferred orientation. Chlorite occurs as cross-cutting plates larger than the surrounding micas. Chlorite is present in the garnet and staurolite zones; the only chlorite seen in either sillimanite zone is associated with cordierite in a single specimen. Chlorite is most abundant in the retrograde zone, where it commonly rims staurolite.

Staurolite is a common mineral of the staurolite and lower sillimanite zones. It occurs as subhedral to euhedral porphyroblasts, locally exhibiting sieve texture due to abundant quartz inclusions. Pelitic layers show twinned crystals on the weathered surface. Staurolite crystals are 2 mm to 2 cm long and show no sign of rotation during growth.

Garnet occurs as subhedral to euhedral grains about 1 mm in diameter. It is present in most pelitic rocks, regardless of grade. Quartz, ilmenite, and graphite inclusions are common and in some cases are so abundant they form a continuous boundary between the rim and core (Boone, 1973, Plate 20B). Garnet in one specimen shows evidence of rotation during growth. Most garnet crystals show postkinematic growth, with very minor rotation or stretching due to late deformation associated with the final stages of metamorphism.

Andalusite is widely distributed throughout the staurolite and lower sillimanite zones and is even seen in some specimens from the upper sillimanite zone. It occurs as large irregular porphyroblasts commonly highly sieved by quartz and micas. Highly sieved cordierite with chlorite rims was found in two specimens (Fig. 2).

Sillimanite occurs in the southern and far western part of the area as fibrolite with biotite and as coarser prismatic crystals. The occurrence of sillimanite contrasts with that of andalusite in that every specimen of the lower and upper sillimanite zones contains sillimanite, while only half of the specimens in the staurolite and lower sillimanite zones contain andalusite (Fig. 2). As discussed in a subsequent section, andalusite and cordierite are believed to be metastable relict minerals from a metamorphic episode previous to the events which produced sillimanite-grade metamorphism in the western and southern parts of the area. (Holdaway has collected a number of upper sillimanite-zone specimens from the Wayne and Fayette 7½-minute quadrangles immediately west of the Augusta 15-minute quadrangle.)

Ilmenite, occurring in every thin section, is the most abundant accessory mineral. Osberg (1974) describes magnetite from Mayflower Hill and Waterville Formation specimens northeast of the area studied. These rocks appear to be marly pelites. To check for magnetite, 12 polished sections of pelites containing opaque minerals were examined on the microprobe using qualitative Ti and Fe analyses. Between 20 and 40 grains were checked on each specimen. Ilmenite was the only opaque oxide.

Graphite occurs in most pelitic rocks as small amounts of finely disseminated specks generally distributed evenly throughout, but it sometimes concentrates in thin layers in an otherwise normal pelitic rock. The presence of graphite is best demonstrated in a polished section by a combination of fine opaque specks when viewed with transmitted light and tiny pits in the same area when viewed with reflected light. Graphite is either less abundant or occurs in larger crystals (or both) in sillimanite-grade rocks. In some specimens one cannot be sure that graphite is present; however, it is never possible to demonstrate its absence in these rocks. Traces of pyrite and/or pyrrhotite are present in most rocks, and chalcopyrite is locally associated with pyrrhotite. Other accessory minerals include tourmaline, apatite, zircon, and rutile.

Mineral analyses

Minerals in twelve polished thin sections (Fig. 2, Table 1) were analyzed with a MAC-400 three-spectrometer automated electron microprobe at Massachusetts Institute of Technology. A 15 kV accelerating potential was used with a 0.03 microampere beam current and a beam diameter of about 2 microns. Muscovite, biotite, staurolite, garnet, chlorite, and cordierite were analyzed for Si, Al, Ti, Fe, Mg, Mn, Zn, Ca, K, Na, and Ba. Silicate standards were used for most of the elements, and analytical data

Table 1. Model analyses of microprobe specimens*

Specimen	147	77	157	AH-1	91	41
Muscovite	3.3	10.5	15.4	5.4	20.5	12.1
Biotite	52.1	38.3	44.0	41.9	27.9	40.5
Garnet	4.1	tr	tr	1.7	4.9	tr
Staurolite	1.5	tr	5.9	0.5	8.0	7.0
Chlorite	tr	7.4	tr	-	-	-
Cordierite	-	-	-	-	-	-
Sillimanite	-	-	-	-	-	1.9
Andalusite	8.0	-	3.6	18.6	12.3	tr
Quartz, plag.	28.9	29.8	27.0	31.5	27.2	37.4
Ilmenite	tr	1.3	2.5	1.2	2.0	tr
Specimen	175	5	102	EW-3	MA-4	107
Muscovite	11.5	30.3	17.5	1.7	7.3	2.2
Biotite	36.3	34.5	20.6	49.4	41.8	39.5
Garnet	-	tr	1.0	tr	1.9	tr
Staurolite	tr	7.6	2.1	1.2	tr	tr
Chlorite	tr	-	-	-	-	-
Cordierite	6.7	-	-	-	-	-
Sillimanite	tr	tr	0.8	2.5	tr	19.4
Andalusite	9.2	4.1	3.1	-	3.8	-
Quartz, plag.	30.1	18.8	53.5	43.5	43.1	36.9
Ilmenite	5.1	3.0	1.4	tr	1.7	tr

*Specimens listed in approximate order of increasing grade. Replacing chlorite not counted. Accessory graphite, apatite, tourmaline, zircon, pyrite, pyrrhotite, and chalcopyrite.

were reduced using the method of Bence and Albee (1968). Each analysis was for 30 seconds or 60,000 counts. Estimated uncertainty is 2 percent of the amount present for major elements and 5 percent for minor elements. All analysis points for a given specimen were within 2 mm of each other. For each mineral except garnet, 1 to 5 grains were analyzed. A total of 3 to 5 analyses of each mineral was averaged. Homogeneity within the analysis area is indicated by average standard deviations for FeO and MgO of 0.25 and 0.10 for biotite, 0.21 and 0.04 for staurolite, 0.30 and 0.24 for chlorite, and 0.21 and 0.09 for cordierite. These figures imply a maximum variation of ±1 mole percent in Fe/(Fe+Mg). For each garnet-bearing rock, a single zoned garnet was analyzed 6 to 10 times at regular intervals across the grain.

Many of the analyzed specimens were collected from the higher grade part of the lower sillimanite zone near the staurolite-out isograd (Fig. 2), and they contain similar mineral assemblages. This was done in order to evaluate compositional effects on Fe–Mg exchange reactions and to estimate the conditions of the lower sillimanite zone. More detailed sampling is needed from adjacent areas in order to define systematic mineralogical changes, but in a general way the minerals show element variation trends which depend on the mineral assemblage and distance from the isograd.

Micas. Chemical analyses of muscovite and biotite are given in Tables 2 and 3 respectively. As noted by Tracy (1978), pelitic muscovites closely approximate the ideal composition with two octahedral cations. Biotites in these high-Al rocks are aluminous in nature and comparable to those analyzed by Guidotti (1974). Because of the prevalence of ilmenite and graphite and the absence of magnetite in the pelitic rocks, most of the Fe in the silicates is assumed to be in the divalent state. A plot of Fe/Mg in biotite *vs.* muscovite (Fig. 3) shows nearly equal distribution between the minerals. Ti tends to concentrate in biotite over muscovite, but both minerals show a slight trend toward Ti enrichment with increasing grade.

Garnet. Garnets were analyzed by making a traverse across a grain with an analysis at least every 150 microns, depending on the size of the grain. Chemical analyses (Table 4) give core and rim compositions. Cores are commonly enriched in MnO relative to rims. Cores range from 8 to 25 mole percent spessartine while rims range from 7.5 to 19 mole percent. Cores are also enriched in grossular and depleted in almandine relative to the rims. Plots of almandine, pyrope, spessartine, and grossular content for two zoned garnets are given in Figure 4.

Staurolite. Staurolite compositions are given in Table 5, with the formula unit based on that of Griffin and Ribbe (1973). The range in Fe/(Fe+Mg) is 0.80 to 0.87. ZnO shows an inverse relationship with the amount of staurolite in the rock (Tables 1, 5), implying that if all the ZnO is in staurolite, the pelitic rocks contain about 0.02% ZnO. The Fe–Mg distribution between staurolite and biotite (Fig. 5) shows a reasonably consistent pattern, suggesting that equilibrium was approached in the specimens analyzed.

Chlorite. Analyses of chlorite are given in Table 6. In all three analyses chlorite has Fe/(Fe+Mg) lower than that of the coexisting biotite, suggesting that it grew in equilibrium with the biotite (Guidotti, 1974).

Fisher (1941) describes a chloritoid phyllite, the locality of which is "one quarter of a mile northwest of the town of Winthrop," and traces it "northward along strike into the Belgrade Lakes area." We have collected many specimens from this area and examined them in thin section, but no chloritoid has been identified. As the area described by Fisher corresponds to the area of retrogressive metamorphism shown in Figure 2, it must be concluded that some of the chlorite was misidentified as chloritoid.

Cordierite. Table 6 gives a single analysis of cor-

Table 2. Chemical analyses of muscovite*

	147	77	157	AH-1	91	41	175	5	102	EW-3	MA-4	107
SiO_2	47.15	47.30	47.17	47.48	46.89	47.07	46.85	46.51	46.77	46.70	45.98	47.13
Al_2O_3	36.77	36.95	35.78	35.55	36.75	36.33	36.36	36.80	36.32	36.68	35.43	35.15
TiO_2	0.37	0.42	0.45	0.37	0.27	0.38	0.39	0.42	0.51	0.54	0.43	0.50
FeO	1.16	1.04	0.98	1.14	0.94	0.87	0.86	0.95	0.96	1.08	1.05	0.71
MgO	0.48	0.50	0.60	0.66	0.45	0.58	0.52	0.44	0.42	0.58	0.72	0.54
MnO	0.00	0.04	0.01	0.00	0.00	0.00	0.00	0.00	0.01	0.00	0.00	0.00
K_2O	9.68	9.71	10.01	9.83	9.83	9.16	9.22	9.02	9.62	9.79	10.11	9.69
Na_2O	1.17	1.12	0.95	0.98	1.29	1.26	1.53	1.51	1.34	0.86	0.86	0.78
BaO	0.49	0.47	0.94	0.25	0.47	0.36	0.97	0.04	0.28	0.44	0.46	0.41
Total	97.27	97.52	96.89	96.26	96.89	95.99	96.70	95.70	96.23	96.67	95.03	94.90
						Formula based on 22 oxygens						
Si	6.131	6.132	6.185	6.228	6.125	6.170	6.139	6.110	6.140	6.092	6.141	6.237
Al	1.869	1.868	1.815	1.772	1.875	1.830	1.861	1.890	1.860	1.908	1.859	1.763
Al	3.766	3.775	3.714	3.725	3.783	3.782	3.755	3.807	3.761	3.757	3.717	3.719
Ti	0.034	0.038	0.042	0.034	0.025	0.035	0.027	0.039	0.049	0.049	0.039	0.039
Fe	0.125	0.110	0.105	0.123	0.100	0.093	0.092	0.102	0.104	0.123	0.113	0.101
Mg	0.091	0.093	0.114	0.127	0.085	0.110	0.099	0.084	0.080	0.107	0.137	0.104
Mn	0.000	0.001	0.000	0.000	0.000	0.000	0.000	0.000	0.000	0.000	0.000	0.000
Σ	4.016	4.017	3.975	4.009	3.993	4.020	3.983	4.032	3.994	4.036	4.006	3.973
K	1.602	1.603	1.671	1.644	1.636	1.530	1.540	1.511	1.608	1.658	1.720	1.635
Na	0.293	9.279	0.241	0.250	0.325	0.318	0.387	0.383	0.337	0.222	0.238	0.267
Ba	0.022	0.002	0.046	0.011	0.022	0.015	0.047	0.001	0.012	0.021	0.023	0.019
Σ	1.917	1.904	1.958	1.905	1.983	1.863	1.974	1.895	1.957	1.901	1.981	1.921
Fe/Fe+Mg	0.579	0.542	0.480	0.492	0.541	0.458	0.482	0.548	0.565	0.535	0.452	0.493
K/K+Na	0.845	0.852	0.874	0.868	0.834	0.828	0.799	0.798	0.827	0.882	0.878	0.860
Assemblage	1a	1	1a	1a	1a	2	2b	2a	2a	2	3a	3a

* Localities and mineral assemblages given in Figure 2. Numbers: analyzed by Novak; letter-number combination: analyzed by Holdaway. Total Fe given as FeO.

dierite which has Fe/(Fe+Mg) of 0.30. The specimen is mineralogically similar to that which occurs at West Sidney in the northeastern part of the Augusta quadrangle (Osberg, 1971), except that the West Sidney locality is near the beginning of the staurolite zone and the present specimen (175) occurs in the lower sillimanite zone (Fig. 2).

Petrologic analysis

Figure 2 shows that the map area can be divided into five types of areas on the basis of the dominant mineral assemblage. These are (1) a garnet zone characterized by garnet without staurolite, (2) a staurolite zone characterized by staurolite without sillimanite, (3) a partly retrograded area of the staurolite zone characterized by chlorite rims on staurolite and locally by retrograde pseudomorphs after staurolite and andalusite, (4) a lower sillimanite zone characterized by sillimanite and staurolite, and (5) an upper sillimanite zone characterized by sillimanite and muscovite with neither staurolite nor K feldspar. The staurolite isograd is not well defined due to poor exposure and will not be discussed in detail. Andalusite may be present in rocks of any grade except presumably those of the garnet zone.

All minerals in pelitic rocks may be described in terms of the system Al_2O_3–FeO–MgO–MnO–H_2O after accounting for the component oxides contained in quartz, muscovite, plagioclase, and ilmenite present in all specimens. In the discussions which follow presence of a fluid phase is assumed.

Most specimens in the staurolite zone contain chlorite. Two assemblages which are widely developed throughout this zone (Fig. 2) are biotite–staurolite–garnet–chlorite and biotite–staurolite–garnet–chlorite–andalusite. Most of the remaining localities are subassemblages of these two. The existence of garnet in these assemblages is consistent with their

Table 3. Chemical analyses of biotite*

	147	77	157	AH-1	91	41	175	5	102	EW-3	MA-4	107
SiO_2	35.63	36.09	36.93	36.21	35.49	36.41	36.57	35.37	34.96	36.24	35.43	36.00
Al_2O_3	19.87	19.58	19.58	19.67	19.64	19.91	19.97	19.74	20.02	20.08	19.62	19.11
TiO_2	1.65	1.75	1.58	1.68	1.64	1.62	1.45	1.64	1.95	2.08	2.20	1.68
FeO	20.06	18.34	17.05	18.25	20.13	17.58	16.77	20.15	21.13	18.32	17.57	17.98
MgO	9.38	10.59	11.26	10.39	9.37	10.78	11.70	9.31	8.29	9.41	9.95	10.51
MnO	0.07	0.14	0.11	0.11	0.04	0.14	0.13	0.06	0.02	0.23	0.14	0.13
K_2O	9.25	9.08	9.26	9.09	9.03	8.80	8.85	9.12	8.67	8.78	9.18	9.22
Na_2O	0.22	0.14	0.18	0.18	0.33	0.32	0.28	0.27	0.32	0.60	0.26	0.26
BaO	0.18	0.12	0.24	0.03	0.10	0.13	0.05	0.04	0.07	0.04	0.03	0.16
Total	96.31	95.70	96.17	95.61	95.77	95.68	95.77	95.70	95.43	95.78	94.37	95.05
					Formula based on 22 oxygens							
Si	5.371	5.411	5.478	5.431	5.376	5.434	5.427	5.359	5.331	5.446	5.386	5.442
Al	2.629	2.589	2.522	2.569	2.624	2.566	2.573	2.641	2.669	2.554	2.614	2.558
Al	0.899	0.868	0.899	0.908	0.881	0.935	0.920	0.888	0.926	1.000	0.902	0.844
Ti	0.185	0.195	0.174	0.189	0.184	0.178	0.160	0.184	0.221	0.242	0.250	0.189
Fe	2.530	2.297	2.114	2.288	2.549	2.193	2.080	2.555	2.693	2.302	2.231	2.271
Mg	2.109	2.365	2.490	2.319	2.116	2.395	2.586	2.103	1.883	2.092	2.254	2.366
Mn	0.008	0.170	0.009	0.013	0.002	0.014	0.014	0.005	0.001	0.013	0.018	0.014
Σ	5.731	5.893	5.686	5.717	5.732	5.715	5.760	5.735	5.724	5.649	5.655	5.684
K	1.777	1.736	1.751	1.738	1.743	1.673	1.673	1.761	1.685	1.678	1.781	1.775
Na	0.061	0.038	0.050	0.048	0.095	0.095	0.078	0.077	0.089	0.041	0.083	0.073
Ba	0.008	0.001	0.011	0.000	0.003	0.005	0.002	0.004	0.003	0.001	0.000	0.007
Σ	1.846	1.775	1.812	1.786	1.841	1.773	1.753	1.842	1.777	1.720	1.864	1.855
Fe/Fe+Mg	0.545	0.466	0.459	0.497	0.546	0.478	0.446	0.549	0.589	0.524	0.497	0.490
K/K+Na	0.967	0.979	0.972	0.973	0.948	0.946	0.956	0.958	0.950	0.976	0.956	0.961
Assemblage	1a	1	1a	1a	1a	2	2b	2a	2a	2	3a	3a

* See Table 2 for notes

high Mn content. The 4-phase assemblage is trivariant [P, T, $X(H_2O)$], while the 5-phase assemblage is divariant and becomes a surface in $P,T,X(H_2O)$ space. Normally such an assemblage would mark an isograd, as a result of the reaction of staurolite, chlorite, and muscovite to biotite, andalusite, and water. However, a simple isograd is not possible in this instance since it must separate areas of biotite–staurolite–garnet–chlorite from areas of biotite–staurolite–garnet–andalusite. If the locally developed cordierite occurrences are considered, the variance is further reduced and there is still no possible pattern of isograds. In our opinion the andalusite and local cordierite represent an earlier metamorphism, at which time some staurolite and garnet formed. Then during a second metamorphism the whole staurolite zone was retrograded as andalusite and biotite reacted to chlorite and more staurolite. With the exception of andalusite and cordierite, all the minerals equilibrated with this later event, as shown by consistent K_D values. The heat source for this second metamorphism was probably to the southeast.

P. H. Osberg (personal communication) has argued for a bed-to-bed variation of $X(H_2O)$ as an explanation for the distribution of mineral assemblages discussed above. During retrograde metamorphism $X(H_2O)$ could drop in the less permeable layers and allow the metastable preservation of andalusite after partial reaction. However, a widespread pattern of large variations in $X(H_2O)$ during a single prograde event appears improbable. Both the staurolite isograd (Osberg, 1968) and the sillimanite isograd (Fig. 2) involve dehydration, and yet each is a very regular feature. The studies of Ferry (1976a, b) demonstrate irregular isograd patterns in impure carbonates, presumably because both H_2O and CO_2 are involved in the equilibria and the calcareous rocks of the area (Fig. 1) are intimately interbedded with pelites. Ac-

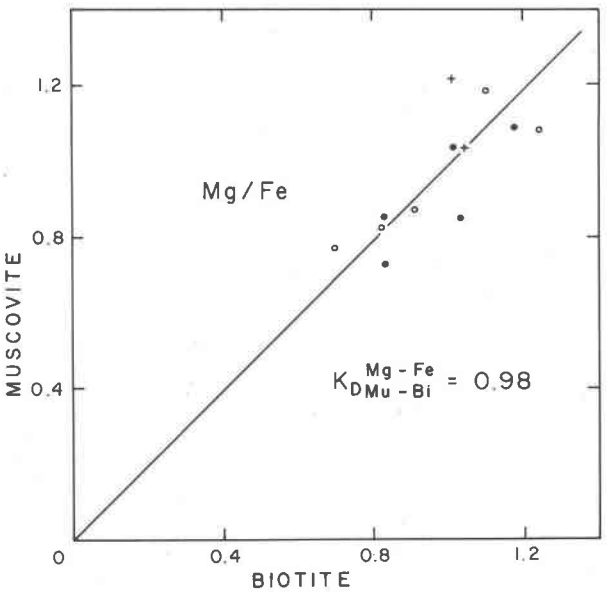

Fig. 3. Mg/Fe K_D plot for muscovite–biotite pairs from the Augusta quadrangle. Dots = staurolite-zone localities, circles = lower sillimanite= zone localities, pluses = upper sillimanite-zone localities. Line gives average K_D.

cording to our model the andalusite isograd of the first metamorphism approximately coincides with the staurolite isograd of the second metamorphism. In the Farmington area to the northwest (Holdaway, Novak and Guidotti, in preparation), the two isograds are clearly distinct.

In the western part of the staurolite zone chlorite is more abundant than elsewhere. The stippled part of Figure 2 is an area in which chlorite is abundant and has textures which clearly indicate its retrogressive origin. As previously indicated for the whole staurolite zone, chlorite cuts across the schistosity formed by muscovite and biotite. In some sections in the retrograde area chlorite plates include smaller staurolite grains. Partial to complete pseudomorphs after staurolite and andalusite are common throughout the area. Toward the northern limits of the retrograded area fine-grained white mica pseudomorphs after andalusite are most common, while staurolite alteration to chlorite is confined to the rims. Euhedral garnets in former andalusite are unaffected. Further south, pseudomorphic reactions after staurolite are more

Table 4. Chemical analyses of garnet*

	147		77		AH-1		91		41		5		102		EW-3		MA-4		107	
	Core	Rim	Core	Rim	Core	Rim	Core	Rim	Core	Rim	Core	Rim	Core	Rim	Core	Rim	Core	Rim	Core	Rim
SiO_2	37.44	37.15	38.30	37.61	37.90	37.43	37.43	37.73	37.51	37.14	37.28	37.14	37.36	37.88	37.50	37.22	36.63	36.93	37.68	37.63
Al_2O_3	21.10	21.06	21.40	21.42	20.36	21.05	20.77	20.95	21.08	20.96	21.30	21.31	20.86	21.01	21.29	21.37	20.90	21.05	19.82	19.41
TiO_2	0.10	0.10	0.02	0.00	0.09	0.00	0.03	0.00	0.03	0.01	0.00	0.00	0.00	0.00	0.01	0.00	0.13	0.13	0.00	0.01
FeO	31.63	34.79	29.16	31.00	28.13	31.11	32.29	34.02	30.80	30.72	32.65	34.56	35.81	36.43	30.17	30.79	26.16	29.27	29.37	29.61
MgO	2.25	2.39	2.63	2.84	2.30	2.54	2.15	2.24	3.20	2.78	2.49	2.31	2.24	2.20	2.65	2.33	2.08	2.72	2.88	2.26
MnO	6.21	3.63	8.35	7.41	8.49	6.37	6.01	3.93	6.79	7.11	5.61	4.68	3.39	3.30	6.28	6.65	11.12	7.97	7.87	8.26
CaO	1.91	1.53	1.69	1.38	2.57	1.89	1.63	1.71	1.04	1.16	1.29	0.77	0.73	0.53	2.39	2.20	2.95	2.20	1.39	1.74
Total	100.63	100.63	100.54	101.65	99.83	100.38	100.30	100.73	100.44	99.87	100.61	100.76	100.40	101.33	100.28	100.54	99.98	100.26	99.01	98.92
Formula based on 12 oxygens																				
Si	2.968	2.987	2.988	2.985	3.049	3.007	3.018	3.022	2.006	3.001	2.991	2.987	3.027	3.027	3.000	2.986	2.967	2.973	3.064	3.082
Al	0.032	0.013	0.012	0.015							0.009	0.013				0.014	0.033	0.027		
Al	1.958	0.981	2.008	1.989	1.929	1.993	1.973	1.977	1.990	1.995	2.004	2.005	1.064	1.978	2.007	2.006	1.962	1.968	1.899	1.871
Ti	0.004	0.005	0.000	0.000	0.037	0.000	0.000	0.000	0.001	0.000	0.000	0.000	0.000	0.000	0.000	0.000	0.006	0.007	0.000	0.000
Σ	1.962	1.986	2.008	1.989	1.966	1.993	1.973	1.977	1.991	1.995	2.004	2.005	1.964	1.978	2.007	2.006	1.968	1.975	1.899	1.871
Fe	2.118	2.337	1.953	2.057	1.893	2.089	2.177	2.278	2.063	2.075	2.190	2.323	2.417	2.434	2.017	2.065	1.772	1.969	1.996	2.028
Mg	0.267	0.287	0.313	0.335	0.275	0.305	0.257	0.283	0.361	0.334	0.296	0.275	0.269	0.261	0.314	0.277	0.250	0.324	0.348	0.275
Mn	0.420	0.245	0.560	0.497	0.578	0.443	0.409	0.265	0.460	0.485	0.380	0.318	0.236	0.222	0.425	0.449	0.762	0.542	0.540	0.572
Ca	0.162	0.131	0.143	0.116	0.220	0.161	0.140	0.145	0.088	0.099	0.109	0.064	0.062	0.044	0.204	0.187	0.255	0.189	0.199	0.151
Σ	2.967	3.000	2.969	3.005	2.966	2.998	2.983	2.971	2.972	2.993	2.975	2.980	2.984	2.961	2.960	2.978	3.039	3.024	3.003	3.026
Mole % Alm	71.4	77.9	65.8	68.5	63.8	69.7	73.0	76.7	69.4	69.3	73.6	77.9	81.0	82.2	68.1	69.3	58.3	65.1	66.6	67.0
Mole % Pyr	9.0	9.6	10.5	11.1	9.3	10.2	8.6	9.5	12.1	11.2	9.9	9.2	9.0	8.8	10.6	9.3	8.2	10.7	11.6	9.1
Mole % Spess	14.2	8.2	18.9	16.5	19.5	14.8	13.7	8.9	15.5	16.2	11.8	10.7	7.9	7.5	14.3	15.1	25.0	17.9	18.0	18.9
Mole % Gross	5.4	4.3	4.8	3.9	7.4	5.3	4.7	4.9	3.0	3.3	3.7	2.2	2.1	1.5	7.0	6.3	8.5	6.3	3.9	5.0
Fe/Fe+Mg	0.888	0.891	0.862	0.860	0.873	0.873	0.894	0.890	0.851	0.861	0.881	0.894	0.900	0.903	0.865	0.882	0.876	0.859	0.852	0.881
Assemblage	1a		1		1a		1a		2		2a		2a		2		3a		3a	

*See Table 2 for notes

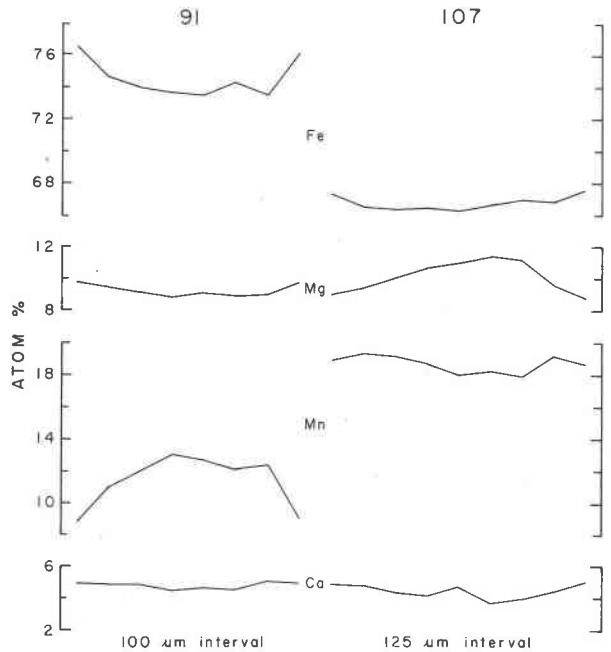

Fig. 4. Rim to rim compositional profiles for 8-fold site contents of garnets from two specimens. Lines connect data points taken at stated intervals. For specimen 91, depletion of Mn + Ca toward rim indicates garnet growth. For specimen 107, increase of Mn + Ca towards rim indicates garnet reaction.

complete, resulting in crystals without fresh surfaces, and consisting of fine-grained muscovite and chlorite. Within the same specimens, fine-grained white mica pseudomorphs after chiastolite or andalusite are found. Chiastolite crystals are confined to very thin graphite-rich layers, similar to those observed by Guidotti and Cheney (1976, Fig. 1). Toward the southern limit of the area, just north of Winthrop, the effects of the retrogressive event appear to be at a maximum. In addition to staurolite, garnet, which was not altered toward the north, has been chloritized by the low-temperature episode. Pseudomorphs maintain the euhedral outline of the host crystals and commonly contain only core remnants of the original mineral. These textures are consistent with a static thermal event accompanied by little deformation. Minor evidence of shearing was noted in a few specimens. West of the retrograde area staurolite-bearing rocks are followed by staurolite–sillimanite rocks with no retrogressive effects.

We interpret the textures of the retrograde area as resulting from the third and latest metamorphic event, with increasing temperature to the west. The parallelism of the western sillimanite isograd with the retrograde area suggests a hinge effect such that in the retrograde area the rocks were being adjusted to lower temperatures while at the western edge of the map area temperature was increasing.

The southern limit of the staurolite zone is defined by the first appearance of sillimanite in trace amounts. The sillimanite isograd, as drawn, separates all pelitic rocks which have staurolite without sillimanite from those which have staurolite and sillimanite. With the exception of a single cordierite–chlorite-bearing rock, chlorite is absent from these rocks. The sillimanite first encountered is of the disharmonious type described by Vernon and Flood (1977), *i.e.*, growing along quartz and plagioclase boundaries at high angles to grain contacts. This implies that the sillimanite grew after equilibrium among grain contacts had been established. As sillimanite increases in amount, much of it grows on or within biotite. Along a zone which approximately coincides with the southern sillimanite isograd are several occurrences of garnet with discontinuous zoning. Such garnets have been interpreted by Boone (1973) as representing more than one stage of garnet growth.

The zone of coexisting sillimanite and staurolite is designated the lower sillimanite zone (Guidotti, 1974). Staurolite, garnet, and andalusite are common throughout the zone in the southern part of the map area. One specimen (Fig. 2) contains cordierite rimmed by chlorite, muscovite, and fine staurolite crystals, which suggests that the cordierite is a relict mineral from an earlier metamorphism. There is no correlation between andalusite and sillimanite occurrence in these rocks. Sillimanite formed as easily in rocks with no andalusite as in rocks containing andalusite. Andalusite becomes more inclusion-filled and skeletal toward the southern edge of the lower sillimanite zone. In some specimens containing both Al silicates, andalusite seems to be selectively replaced by large muscovite grains, as was observed by Chinner (1973). Staurolite also decreases in modal abundance toward the southern limit of the zone.

The upper sillimanite zone in the southern part of the area is characterized by the absence of staurolite, the near absence of andalusite, and a marked increase in modal sillimanite. Toward the southern limit of staurolite stability, coarse-grained biotite and muscovite pseudomorphous after staurolite are common. Locally only traces of Zn-rich staurolite remain (Tables 1, 5), and these are completely engulfed within large (0.3 mm) grains of muscovite. In contrast to pseudomorphs previously described, this mineral replacement is prograde in nature (Guidotti, 1968). The mineral assemblage sillimanite–alman-

Table 5. Chemical analyses of staurolite*

	147	77	157	AH-1	91	41	175	5	102	EW-3
SiO_2	27.17	27.97	28.13	28.52	28.08	28.03	28.05	27.64	28.19	28.53
Al_2O_3	54.70	54.43	52.88	52.95	54.11	54.86	53.87	54.77	54.05	55.86
TiO_2	0.31	0.52	0.59	0.50	0.50	0.58	0.55	0.58	0.55	0.50
FeO	13.99	12.11	13.13	13.10	13.95	12.93	12.47	14.35	13.38	10.58
MgO	1.41	1.56	1.60	1.61	1.43	1.61	1.76	1.43	1.36	0.88
MnO	0.15	0.38	0.61	0.29	0.15	0.42	0.44	0.24	0.15	0.42
ZnO	0.72	1.80	0.43	1.02	0.37	0.18	1.08	0.34	0.47	1.16
Total	98.54	98.79	97.35	97.99	98.58	98.61	98.20	99.35	98.15	98.00
					Formula based on 47 oxygens					
Si	7.690	7.859	8.011	8.076	7.909	7.855	7.921	7.748	7.956	7.992
Al	0.310	0.141			0.091	0.145	0.079	0.252	0.044	0.008
Al	17.937	17.887	17.757	17.692	17.873	17.976	17.854	17.853	17.938	18.396
Ti	0.066	0.107	0.123	0.100	0.102	0.119	0.111	0.118	0.114	0.098
Σ	18.003	17.994	17.880	17.692	17.975	18.095	17.965	17.971	18.052	18.494
Fe	3.305	2.845	3.127	3.102	3.280	3.029	2.943	3.361	3.158	2.469
Mg	0.589	0.651	0.677	0.674	0.597	0.666	0.737	0.594	0.568	0.360
Mn	0.033	0.090	0.142	0.066	0.031	0.097	0.099	0.054	0.031	0.098
Zn	0.149	0.371	0.086	0.207	0.071	0.031	0.219	0.066	0.093	0.237
Σ	4.076	3.957	4.031	4.049	3.979	3.823	3.998	4.075	3.850	3.164
Fe/Fe+Mg	0.849	0.814	0.822	0.822	0.846	0.820	0.800	0.850	0.848	0.873
Assemblage	1a	1	1a	1a	1a	2	2b	2a	2a	2

* See Table 2 for notes.

dine–biotite–muscovite–quartz–plagioclase–ilmenite is ubiquitous in the upper sillimanite zone (Fig. 2).

We interpret the lower and upper sillimanite zones as the result of the second metamorphism to affect the area. Thermal gradients here increased to the southeast. The absence of a well-defined zone of extensive retrograde metamorphism parallel to the southern sillimanite isograd suggests that (1) staurolite-zone conditions were much more widespread during this second metamorphism than during the third metamorphism which affected the rocks along the western edge of the area, and (2) the rocks were already hot at the inception of the second metamorphism, which implies a relatively short time span between the first and second metamorphic episodes.

To summarize, much of the area was affected by an early metamorphism which produced andalusite, garnet, staurolite, and some cordierite. A second metamorphism partly destroyed cordierite and partly converted andalusite–biotite to staurolite–chlorite in the central and northern part of the area, and up-

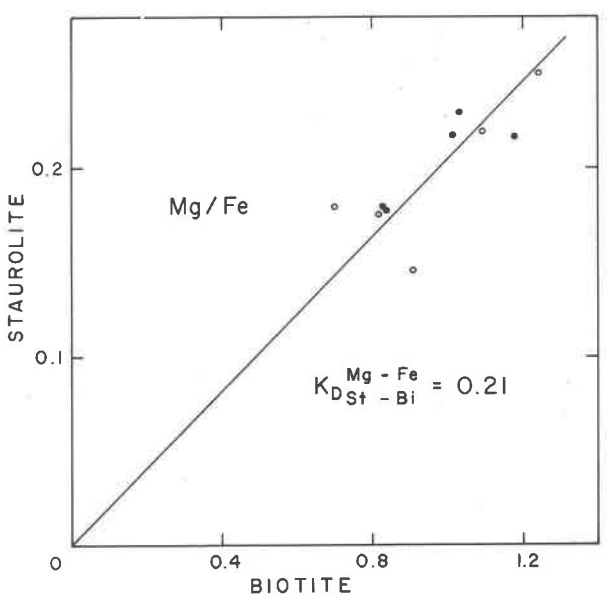

Fig. 5. Mg/Fe K_D plot for staurolite–biotite pairs from the Augusta quadrangle. Dots = staurolite zone, circles = lower sillimanite zone. Line gives average K_D.

Table 6. Chemical analyses of chlorite and cordierite*

	Chlorite			Cordierite
	77	157	175	175
SiO_2	25.01	25.93	25.45	49.04
Al_2O_3	23.17	22.74	23.76	32.82
TiO_2	0.08	0.07	0.01	0.03
FeO	23.10	21.55	20.26	6.36
MgO	16.04	16.79	18.21	8.37
MnO	0.24	0.26	0.18	0.32
Na_2O	-	-	-	0.80
Total	87.63	87.34	87.86	97.74
	Formula based on 28 oxygens			18 oxygens
Si	5.197	5.336	3.192	5.035
Al	2.803	2.664	2.808	0.965
Al	2.873	2.851	2.903	3.006
Ti	0.009	0.008	0.000	0.001
Fe	4.013	3.709	3.453	0.544
Mg	4.970	5.153	5.533	1.279
Mn	0.038	0.044	0.028	0.026
Na	-	-	-	0.157
Σ	11.903	11.765	11.917	5.013
Fe/Fe+Mg	0.447	0.419	0.384	0.300
Assemblage	1	1a	2b	2b

* See Table 2 for notes.

graded rocks in the southern part to sillimanite grade. A third metamorphism produced a NNE-trending zone of more extensive retrogressive effects and upgraded the western edge of the area. In the discussions which follow, the presence of andalusite or cordierite interpreted to be relict will be ignored.

Garnet zoning and mineral reactions

J. B. Thompson (1957) first introduced the concept of defining isograds on the basis of discontinuous reactions, in order to minimize original bulk-compositional effects. The applicability of this concept has been repeatedly demonstrated in the field (*e.g.*, Green, 1963; Albee, 1968; Carmichael, 1970). Winkler (1979, p. 66) further emphasizes this point and uses the term reaction-isograd. Index-mineral-defined isograds in the classical sense are still useful for providing a general framework for establishing metamorphic conditions, but a knowledge of specific reactions is necessary in order to deduce the complete metamorphic history of an area.

In addition, detailed chemical analyses of minerals provide evidence for continuous reactions (Thompson, 1957) in which no change in the mineral assemblage is apparent. Garnet zoning patterns add another dimension to the understanding of continuous reactions. Because diffusion in garnets is slow under medium-grade conditions (Tracy *et al.*, 1976), a continuous record of element distribution with time is preserved. This distribution, along with the Fe–Mg–Mn variation of the other mineral species, is used here to deduce the important equilibria and mineral reactions, both continuous and discontinuous.

Garnet zoning

Figure 6 shows an AFM plot which includes the total range of garnet rim composition in terms of Fe/(Fe+Mg). The limiting points also exhibit the maximum range of spessartine and grossular components for rims (Table 4). This maximum range is encompassed in specimens which contain sillimanite and staurolite, but the range in Fe/(Fe+Mg), spessartine, and grossular components is comparable in the staurolite-zone rocks. The garnets as a whole are characterized by (1) an absence of compositional trends as a simple function of grade, (2) a tendency toward higher Fe/(Fe+Mg) in garnet with lower spessartine plus grossular component, and (3) depletion in spessartine plus grossular from core to rim accompanied by little change or slight increase in Fe/(Fe+Mg). Because garnet is the main carrier of Mn, the reduction in Mn from core to rim suggests that in

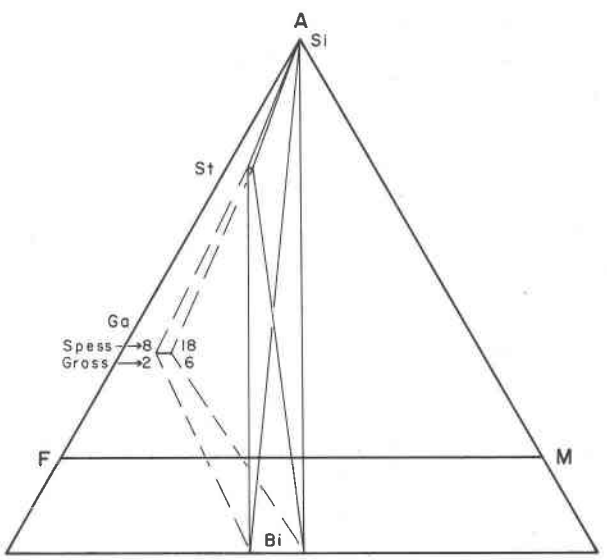

Fig. 6. AFM plot giving extremes of garnet rim composition stable with sillimanite, staurolite, and biotite. As shown, spessartine and grossular contents are highest in low-Fe garnets and lower in high-Fe garnets. The ranges shown for minerals are also applicable to the staurolite zone.

most instances garnet was growing during equilibration of the rim (Tracy *et al.*, 1976). Figure 7 gives a schematic pressure–temperature diagram for equilibria involving almandine, biotite, staurolite, muscovite, and sillimanite. If we assume that the rocks all crystallized at about the same pressure, then the presence of garnet–muscovite–biotite–staurolite in the rocks requires that the sum of spessartine and grossular decrease as Fe/(Fe+Mg) increases, in order for conditions to stay approximately parallel to the nearly flat curve for

Staurolite + Biotite ⇄ Almandine
+ Muscovite + H_2O[2] (1)

Once sillimanite is produced, two additional equilibria must prevail:

Staurolite + Muscovite ⇄ Biotite
+ Sillimanite + H_2O (2)

Staurolite ⇄ Sillimanite + Almandine + H_2O (3)

As staurolite breaks down over a temperature range, equation 2 requires that all minerals become more Fe-rich because Mg fractionates more strongly into biotite than into the other minerals. At the same time, more garnet is being produced and its spessartine and grossular contents must decrease to maintain equilibrium for equation 1. In summary, the relationship between Fe/(Fe+Mg) and the sum of spessartine and grossular in garnet must hold for all but the two highest-grade specimens which have no staurolite. However, once sillimanite begins to form, each garnet must increase in Fe/(Fe+Mg) and decrease in spessartine and grossular as temperature rises. For these rocks, the composition of garnet is a bulk-compositional effect related to Fe/(Fe+Mg) of the dominant biotite and to temperature, once sillimanite has formed. Finally, because all but two of the rocks contain staurolite, garnet grows during increasing temperature. The continuous reaction

Almandine + Muscovite ⇄ Biotite + Sillimanite (4)

must remain at equilibrium but cannot begin to destroy garnet until all the staurolite has reacted. The facts that Mn depletion requires garnet growth and that garnet growth is a prograde phenomenon in these rocks indicate that the garnet rims are in most cases prograde effects.

[2] Quartz is omitted from all reactions for simplicity.

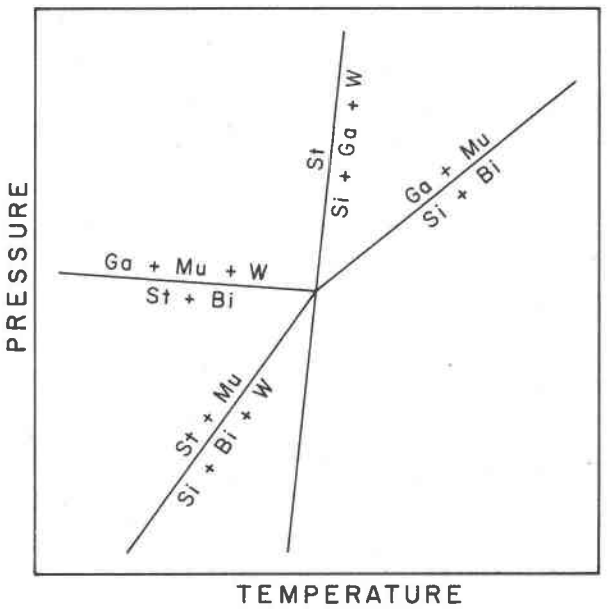

Fig. 7. Schematic pressure–temperature diagram for the system $FeO–Al_2O_3–SiO_2–K_2O–H_2O$ involving excess-SiO_2 and excess-H_2O reactions about the invariant point involving garnet–biotite–staurolite–muscovite–sillimanite. Relative slopes are based on data of Thompson (1976).

Discontinuous reactions

The isograds of Figure 2 may each be related to a particular discontinuous reaction. The absence of chloritoid in the region supports a reaction such as

Almandine + Chlorite + Muscovite ⇄
Staurolite + Biotite + H_2O (5)

for the first appearance of staurolite. Based on other areas (Osberg, 1968; Guidotti, 1970b) the first appearance of staurolite is at a more or less constant grade, but almandine and chlorite can persist together to higher temperatures due to Mn and Ca in the garnet.

The first sillimanite must form by the reaction

Staurolite + Chlorite + Muscovite ⇄
Biotite + Sillimanite + H_2O (6)

as implied by AFM topologies on either side of the sillimanite isograd (Guidotti, 1974). In chlorite-free rocks and in rocks where chlorite has reacted away, sillimanite forms by the continuous reaction 2. Reaction 6 is sharply defined in the field (Fig. 2) and results in the immediate disappearance of chlorite. The reaction

Andalusite ⇄ Sillimanite (7)

is not considered responsible for the *first* appearance

Table 7. Garnet–biotite K_D temperature estimates

Specimen	Mineral	X_{Fe}/X_{Mg}	K_D	T°C*	T°C+
147	Garnet core	7.933	6.613	521	523
	Garnet rim	8.143	6.786	515	516
	Biotite	1.200			
77	Garnet core	6.240	6.424	528	532
	Garnet rim	6.140	6.322	532	537
	Biotite	0.971			
AH-1	Garnet core	6.884	6.977	509	508
	Garnet rim	6.849	6.942	510	509
	Biotite	0.987			
91	Garnet core	8.471	7.032	507	505
	Garnet rim	8.050	6.682	519	520
	Biotite	1.205			
41	Garnet core	5.715	6.241	535	541
	Garnet rim	6.213	6.785	515	516
	Biotite	0.916			
5	Garnet core	7.399	6.090	541	549
	Garnet rim	8.447	6.953	510	509
	Biotite	1.215			
102	Garnet core	8.985	6.282	533	539
	Garnet rim	9.326	6.521	525	527
	Biotite	1.430			
EW-3	Garnet core	6.424	5.838	551	562
	Garnet rim	7.455	6.775	516	516
	Biotite	1.100			
MA-4	Garnet core	7.088	7.161	503	500
	Garnet rim	6.077	6.140	539	546
	Biotite	0.990			
107	Garnet core	5.736	5.976	545	555
	Garnet rim	7.375	7.683	492	481
	Biotite	0.960			

$$K_D = \frac{X_{Fe}^{Ga}}{X_{Mg}^{Ga}} \Big/ \frac{X_{Fe}^{Bi}}{X_{Mg}^{Bi}}$$

* Thompson (1976)

\+ Ferry and Spear (1978)

of sillimanite for the following reasons: (1) Texturally, sillimanite appears to be a product of a later metamorphic episode, as shown by its growth along undisturbed quartz and plagioclase boundaries. (2) Andalusite and sillimanite are rarely seen in contact, and when they are, sillimanite needles cut across preexisting andalusite crystals, leaving them undisturbed with no sign of a reaction relationship (Vernon and Flood, 1977, Fig. 1a). (3) The zone of discontinuously zoned garnets near the southern sillimanite isograd is consistent with more than one period of metamorphism. (4) The decrease in staurolite and disappearance of chlorite are consistent with reaction 6. (5) Sillimanite appears in andalusite-free rocks at the same grade as it appears in andalusite-bearing rocks. Andalusite is gradually converted to sillimanite throughout the lower sillimanite zone and the beginning of the upper sillimanite zone.

Staurolite disappears by the reaction

$$\text{Staurolite} + \text{Muscovite} \rightleftarrows \text{Biotite} + \text{Sillimanite} + \text{Garnet} + H_2O \qquad (8)$$

the combination of reactions 2 and 3. However, this reaction is not strictly discontinuous, due to Mn and Ca in the garnet. These minerals coexist in most rocks once sillimanite has formed. As temperature rises, reaction 2 dominates and progressively increases Fe/(Fe+Mg) in all minerals (Fig. 7). As reaction progresses the growing garnet becomes depleted in spessartine and grossular until staurolite eventually disappears. Once staurolite has reacted away, the continuous reaction 4 may occur. A few thin sections of highest-grade rocks show reaction of garnet by pseudomorphs of biotite or biotite and sillimanite after garnet.

Conditions of metamorphism

Estimates of temperature and pressure for the Augusta area during the last metamorphism were made with the intent of avoiding use of any of the Al_2SiO_5 triple points, due to the lack of complete agreement on this system.

Garnet–biotite K_D

The ubiquitous presence of biotite and garnet in the pelitic rocks allows the use of the recently calibrated geothermometer based on Fe–Mg partitioning in natural assemblages (Thompson, 1976) as well as in synthetic phases (Ferry and Spear, 1978). For the temperature range involved here (Table 7), the two calibrations agree quite well.

Garnet rim compositions were measured about 5 microns from the actual rim to avoid effects of grain curvature from differential hardness during polishing. These determinations involve the assumption that the core garnet equilibrated with biotite of the same composition as that now in the rock (Tracy *et al.*, 1976). Biotite is the dominant Fe–Mg phase, being 6 to 25 times as abundant as garnet and 3.5 to 35 times as abundant as staurolite (Table 1). Ilmenite components dissolving in the biotite with increasing temperature might be expected to drive the biotite toward slightly more Fe-rich compositions with increasing grade. More important is the Fe enrichment which should result as staurolite begins to break down in the lower sillimanite zone. This implies that core temperatures from the sillimanite zone are probably maximum values. Large changes in biotite composition are not possible within a single specimen, because the relatively small amounts of staurolite

must disappear before having a major effect on biotite composition. Valid geothermometry also requires complete diffusion in biotite if it changes composition and absence of diffusion in garnet as it changes composition. The absence of zoning in biotite and the generally reasonable temperature values (Table 7) suggest that this is a good approximation.

A 1 mole percent change in biotite Fe/(Fe+Mg) changes temperature by about 10° while a 1 mole percent change in garnet Fe/(Fe+Mg) changes temperature by about 20°. Thus analytical error introduces a potential ±30° uncertainty while calibration error adds another ±20°.

Temperature plots may be made for each point of an analytical traverse across a garnet. Such plots given in Figure 8 show a prograde and a retrograde profile. Analysis of the data of Table 7 in light of the above discussion, and the fact that Mn+Ca depletion toward rims results from prograde growth, indicates that all but four of the garnets showed approximately level or increasing temperature during growth. Three specimens, 41, EW-3, and 107 have retrograde rims as indicated by Mn+Ca increase, and core to rim temperature decrease of 25° to 74°. Specimen 5 shows a retrograde K_D and a prograde Mn+Ca change. This could have resulted from retrograde Fe–Mg exchange (Tracy *et al.*, 1976). The average temperature of the staurolite zone was 519±12°C[3] including core and rim temperatures, 521±12°C including only rim temperatures. The average temperature for the lower sillimanite zone was 528±20°C including cores and rims, 537±13°C including rims only. The four retrograde rims were excluded. For comparison, Osberg estimated a temperature of 500°C for the West Sydney locality in the staurolite zone (Osberg, 1971) and 550°C for the sillimanite isograd (Osberg, 1974).

The fluid phase

Among other important variables which affect the conditions of metamorphism is the composition of the fluid phase. This is an especially important variable in graphite-bearing pelitic rocks in which the water expelled during progressive dehydration reactions becomes diluted with other species, mainly CH_4, CO_2, H_2, and CO (French, 1966), thus lowering $P(H_2O)$ and affecting the physical stability ranges of mineral assemblages (see for example Holdaway, 1978).

In our treatment we assume P(fluid) = P(total).

[3] One standard deviation of data, Ferry and Spear calibration.

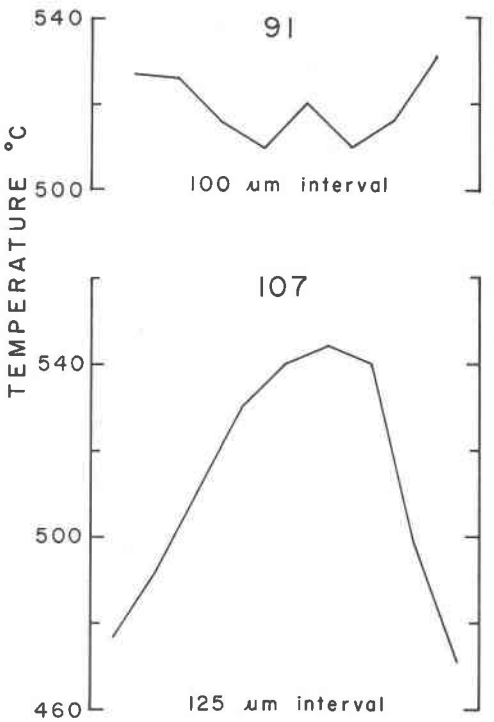

Fig. 8. Rim to rim temperature profiles for the garnets shown in Fig. 4. Specimen 91 shows prograde rims while specimen 107 shows retrograde rims. Note that the core temperatures for specimen 107 in the sillimanite zone could have been affected by changing biotite composition (see text).

Important reactions to consider are (Eugster and Skippen, 1967):

$$C + O_2 \rightleftarrows CO_2 \quad (9)$$

$$CO + \tfrac{1}{2}O_2 \rightleftarrows CO_2 \quad (10)$$

$$H_2 + \tfrac{1}{2}O_2 \rightleftarrows H_2O \quad (11)$$

$$CH_4 + 2O_2 \rightleftarrows CO_2 + 2H_2O \quad (12)$$

With independent estimates of temperature and pressure, the amounts of the diluting gas species can be calculated. Data for equilibrium constant calculations were taken from Ohmoto and Kerrick (1977, Table 1). Fugacity coefficients used are from the following sources: H_2, CO, CH_4, Ryzhenko and Volkov (1971); CO_2, Zharikov *et al.* (1977); H_2O, Burnham *et al.* (1969). QFM buffer data are from Huebner (1971).

As a first approximation, calculations were made using an average temperature of 550°C for the staurolite-out isograd (Table 7) and a total pressure estimate of 4.0 kbar, approximating the maximum pressure estimate of Ferry (1967a) for the Waterville–Vassalboro area. Partial pressures of the various

Table 8. Partial pressures of gas species with graphite, 550°C, 4000 bars

Gas	γ*	$P_{CO_2} = P_{CH_4}$	f_{O_2} = QFM
H_2O	0.459	3465 bars	3327 bars
CO_2	4.19	260 bars	547 bars
CH_4	4.05	260 bars	115 bars
H_2	2.04	13.5 bars	9 bars
CO	3.59	1.5 bars	2 bars
O_2		$f_{O_2} = 10^{-22.15}$ atm	$f_{O_2} = 10^{-21.83}$ atm
X_{H_2O}		0.866	0.830

* See text for references

gas species were then calculated by solving the above gas equations simultaneously on two different assumptions. One set of determinations assumes equal molar production of CH_4 and CO_2 by the reaction:

$$2C + 2H_2O \rightleftarrows CO_2 + CH_4 \qquad (13)$$

which yields a maximum estimate for $X(H_2O)$ (French, 1966). A second calculation was done at QFM (quartz–fayalite–magnetite) buffer conditions, similar to those found by Osberg (1971) in the Waterville–Vassalboro area for coexisting ilmenite and magnetite. Calculated partial pressures of the gas species are shown in Table 8 along with $X(H_2O)$. The sulfur fluid species have been omitted due to sporadic occurrence of sulfides. However, sulfur species could have locally produced lower values of $X(H_2O)$. Ideal mixing in the fluid phase has been assumed, following Ohmoto and Kerrick (1977).

Reactions involving staurolite

From the maximum value of $X(H_2O)$ given in Table 8 and two lower values of 0.80 and 0.75, an approximation of the P-T conditions was made for lower sillimanite zone rocks based on two different experimentally determined reaction equilibria. The two sets of mineral equilibrium data which are applicable to rocks of the Augusta area are:

$$\text{Staurolite} \rightleftarrows \text{Sillimanite} + \text{Almandine} + H_2O \qquad (3)$$

as determined by Richardson (1968), and the

$$\text{Staurolite} + \text{Muscovite} \rightleftarrows \text{Biotite} + \text{Sillimanite} + H_2O \qquad (2)$$

reaction boundary of Hoschek (1969). Both curves can be adjusted for mineral composition and $X(H_2O)$. The intersection of the two reaction curves defines a unique point in P-T space for a given set of mineral compositions and value of $X(H_2O)$, assuming $P(\text{total}) = P(\text{fluid})$. If a fluid phase was non-existent or $X(H_2O)$ was less than the values assumed here, then these estimates will be the maximum values of temperature and pressure (Table 11) possible for the conditions of metamorphism. Reaction 3 has been studied in the pure Fe system with $P(H_2O) = P(\text{total})$, thus both mineral solid solution and dilution of the fluid phase will have an effect on actual stability relations in the natural system. Mineral compositions used by Hoschek (1969) approximate those determined by microprobe analyses for this study. Reaction 2 has therefore been adjusted for dilution of the fluid phase only. Reaction boundaries may be adjusted with a temperature or a pressure shift.

Temperature adjustments for reaction 3 were made using the relationship:

$$T(2) - T(1) = \Delta T(a) = RT(2)\ln K/\overline{\Delta S} \qquad (14)$$

for assumed ideal solid solutions in mineral species and:

$$T(3) - T(2) = \Delta T(b) = RT(3)\ln X''(H_2O)/\overline{\Delta S} \qquad (15)$$

for the fluid phase (Holdaway, 1978). $T(1)$ is the initial temperature for each reaction while $T(2)$ and $T(3)$ are the final temperatures after mineral and fluid composition adjustments respectively. $X''(H_2O)$ is the mole fraction of water raised to the number of moles of water in the balanced reaction.

In a similar fashion, reaction 2 was adjusted in pressure using the relation:

$$P(2) - P(1) = \Delta P = -RT\ln X''(H_2O)/\Delta V \qquad (16)$$

Entropy values were calculated following the procedure of Holdaway (1978). Molar volume data are mainly from Robie *et al.* (1978) and Burnham *et al.* (1969). Entropy and volume data are shown in Table 9 along with ΔS for reaction 3 and ΔV for reaction 2. The calculated changes in pressure and temperature are given in Table 10 for each reaction, with an example for specimen 102 shown diagrammatically in Figure 9. The intersections of reactions 2 and 3 (reaction 8) for all specimens containing graphite are shown in Table 11 for three different values of $X(H_2O)$.

These calculations show that in the lower sillimanite zone temperature estimates vary from about 590°C at $X(H_2O) = 0.75$ to a maximum of 655°C at $X(H_2O) = 0.866$. At these same conditions pressure estimates range from 3.2 to 5.1 kbar. These values are in good agreement with the P–T estimates of Guidotti (1970a) for the lower sillimanite zone.

Interpretation of results

Previous estimates of the pressure–temperature relationships in the Augusta–Vassalboro area by Osberg (1974) and Ferry (1976b) have relied on the use of the aluminum silicate triple-point diagram as determined by Holdaway (1971). Although Holdaway's slope for the andalusite–sillimanite transition has been found to be most consistent with thermochemical data (Anderson *et al.*, 1977), use of the Al_2SiO_5 polymorphs to accurately estimate pressures of metamorphism may be inaccurate (A. B. Thompson, 1976). The andalusite–sillimanite transformation is known for its sluggish nature, which allows andalusite to persist unreacted well outside of its field of stability. Also, as postulated here, sillimanite is probably the product of a later metamorphism at higher pressures than the andalusite-producing event. During this later metamorphism the pressure may have been higher due to increased overburden at a later time.

For these reasons, one might consider the 550°C, 2.8 kbar estimates of Osberg (1974) for his sillimanite isograd to be lower limits of temperature and pressure for the Augusta area. A maximum pressure estimate in the 550°–600°C range, based on absence of kyanite, would be between 4.5 and 6.0 kbar (Newton, 1966; Richardson *et al.*, 1969; Holdaway, 1971).

As shown, the procedure used to estimate *P–T* conditions in this study is subject to variations in $X(H_2O)$. Ferry (1976b) notes that $X(H_2O)$ can be expected to vary on a bed-to-bed scale, due to fluid compositional differences resulting from proximity to sources of CO_2 and H_2O such as interbedded carbonate-bearing layers and granitic intrusions respectively. Even among the samples studied in detail, some were characterized by absence of clearly detectable graphite, which further suggests that fluid compositional differences can exist on any scale.

Abundant pegmatites throughout the area suggest that the magmas generating the various plutons were water-saturated. The spatial relationship between zoisite in the carbonate rocks and the outcrop pattern of plutons (Fig. 1) also suggests the presence of a water-rich fluid, as zoisite-bearing rocks are indicative of a water-rich environment (Kerrick, 1974). Thus if QFM conditions were approximated, the distribution of the fluid species could not have varied significantly from those shown in Table 8.

Considering the errors involved, the agreement between the garnet–biotite geothermometry and the temperatures indicated from staurolite equilibrium studies is reasonable. Values of $X(H_2O)$ less than 0.70

Table 9. Entropy and volume data*

Mineral	$S_{900°K}$ (J/°K)	Volume (J/bar)
Quartz	108.35	2.2688
Fe Staurolite	1492.22[a]	22.8146[c]
Almandine	803.96[a]	11.5282[d]
Sillimanite	274.91	4.9900
Water (4000 bars)	143.26[b]	2.3774[b] (873°K)
Muscovite		14.0710
Fe Biotite		15.4467[e]

6 Staurolite + 11 Quartz = 4 Almandine + 23 Sillimanite + $6H_2O$ (3)

6 Staurolite + 4 Muscovite + 7 Quartz = 31 Sillimanite + 4 Biotite + $6H_2O$ (2)

ΔS_3 = 253.16 J/°K

ΔV_2 = 21.689 J/bar

* Data from Robie et al. (1978) except where indicated

a Structural analog method, Holdaway (1978)

b Burnham et al. (1969), 4000 bars

c Griffin and Ribbe (1973) times 47/46 (see Holdaway, 1978).

d Skinner (1956)

e Hewitt and Wones (1975)

Table 10. Temperature and pressure shifts for reactions 3 and 2

Specimen	Reaction	ΔT_a	ΔT_b at 4000 bars X_{H_2O} = 0.866	X_{H_2O} = 0.80	X_{H_2O} = 0.75
41	3	-47	-25	-38	-49
5	3	-41	-25	-38	-49
102	3	- 5	-26	-40	-51
EW-3	3	-48	-25	-38	-49

		X_{H_2O}	ΔP at 873°K
all specimens	2	0.866	+289
	2	0.80	+448
	2	0.75	+578

ΔT_a: effect of mineral composition

ΔT_b: effect of dilution of water

Estimated error in ΔT and ΔP is 25%

Table 11. Intersections of reactions 2 and 3*

Specimen	X_{H_2O} 0.866	0.80	0.75
41	3.8 kb 607°C	3.4 kb 592°C	3.1 kb 580°C
5	5.5 kb 656°C	5.1 kb 640°C	4.8 kb 628°C
102	4.0 kb 614°C	3.6 kb 599°C	3.3 kb 587°C
EW-3	3.7 kb 605°C	3.3 kb 590°C	3.0 kb 578°C

* Data from Table 10 and experimental stability curves for X_{H_2O} = 1, shown in Figure 9.

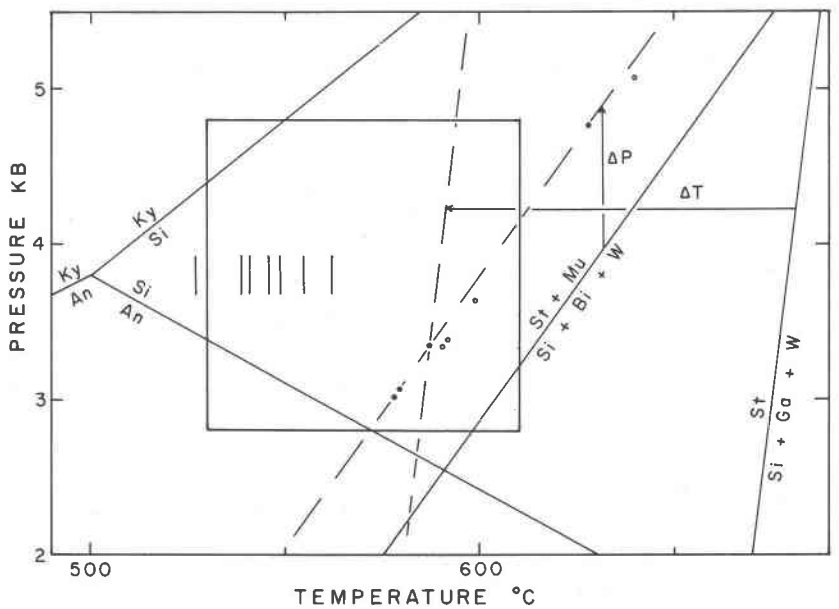

Fig. 9. Intersections of reactions 2 and 3 adjusted for mineral and fluid phase compositions (Table 11) and garnet–biotite geothermometry results for the lower sillimanite zone (Table 7). Dots = conditions for $X(H_2O) = 0.75$, circles = conditions for $X(H_2O) = 0.80$, vertical lines = garnet–biotite temperatures, box = overall estimate, including error, for lower sillimanite-zone conditions. Dashed lines show corrected curves for reactions 2 and 3 applicable to specimen 102 at $X(H_2O) = 0.75$. Reactions at $X(H_2O) = 1$ are based on Richardson (1978) and Hoschek (1979) modified by Winkler. Aluminum silicate diagram is that of Holdaway (1971).

place all the intersections in the andalusite stability field for any Al silicate determination. Temperatures above 600°C are inconsistent with those obtained by Cheney and Guidotti (1979) for the sillimanite–K feldspar zone in the Puzzle Mountain area, NW Maine. Such conditions are not realized within the Augusta Quadrangle.

Combining all methods of P–T determination, a best average estimate for the lower sillimanite zone is $X(H_2O) = 0.75 \pm 0.10$, $P = 3.8 \pm 1$ kbar, $T = 570 \pm 40$°C. Thus, the Holdaway (1971) triple point appears most consistent with the pressure–temperature conditions estimated for the Augusta area. The small temperature discrepancies between the two methods and the need for $X(H_2O)$ somewhat less than calculated (Table 8) suggest that the available staurolite experimental results may be 25 to 50° too high.

Conclusions

Regional relationships

The metamorphism observed in the Augusta area has several characteristics in common with the various episodes described by Guidotti (1970b), suggesting the possibility that at least a few of the events were coeval or similar in style in the two areas. Some of the similarities include the observations that:

(1) pseudomorph-producing events are similar;

(2) cordierite is rimmed by coarse chlorite, suggesting it is a metastable relict from a previous event, possibly coeval with andalusite;

(3) isograds, both prograde and retrograde, are spatially related to the distribution of igneous bodies;

(4) sillimanite appears to be the result of a later metamorphic episode, also related to the outcrop pattern of plutons.

Guidotti's M(2) event is an andalusite–biotite–staurolite-producing event, and, like the one in the Augusta area, its origin is uncertain. Possibly andalusite and locally cordierite were the result of a widespread (lower pressure) event, the effects of which were expressed on a regional scale. M(3) (Guidotti) is represented in the Augusta area by two later sillimanite-producing events closely associated with the distribution of plutons, but which further from the contacts become staurolite–biotite-chlorite events, which begin to destroy andalusite and cordierite.

Dallmeyer and Vanbreeman (1978) suggested that the sillimanite-grade rocks are indicative of a higher pressure regime. They cite a regional southwest reduction in $^{40}Ar/^{39}Ar$ mineral ages as being due largely to differences in metamorphic grade, the younger ages corresponding to higher grades and longer cooling periods. (Zartman *et al.*, 1970, had previously explained the younger ages as the result of

a Permian thermal event.) The concordance of mineral ages between plutons and high-grade country rocks suggests to Dallmeyer and Vanbreeman that these plutons, which include the Hallowell pluton near Augusta, were emplaced at deeper crustal levels than those which intrude lower-grade rocks farther to the north. Though this may be the case, there are other factors to consider. One of these includes the hypothesis postulated here that the sillimanite-grade metamorphism represents *later* metamorphic episodes, associated with higher pressures. Mineral ages could have been partly to totally reset due to these later events, whose heat sources were located to the west and southeast.

Other evidence which suggests that the sillimanite overprint was possibly at higher pressures relative to the other events in the area involves the character of the sillimanite-producing events. The sillimanite-producing event whose source was located to the west of the town of Winthrop produced a widespread area of retrogression which included the production of staurolite and andalusite pseudomorphs along with the formation of large amounts of chlorite. The sillimanite isograd to the southeast shows only minor retrograde products. For this reason, the two sillimanite isograds are believed to have been produced separately, and seem related only because they intersect southwest of Winthrop. In fact, the geometry of the sillimanite isograd alone suggests that more than one metamorphic episode was involved in its formation. The amount of retrogression associated with the event to the west suggests that the country rocks affected were cooler than those affected by the southern event, implying that the southern event more closely followed M(2) than the western event.

Cause of metamorphism

Several of the igneous bodies in western and southern Maine, including the Mooselookmeguntic pluton and the Sebago pluton, have been proposed to be subhorizontal sheets as opposed to bulbous or cylindrical masses (Kane and Bromery, 1968; Moench and Zartman, 1976). Kane *et al.* (1972) and Nielsen *et al.* (1976) have correlated these sheet-like bodies with regions of high-grade rocks, and suggested that their shapes result from rheological properties of the rocks at high temperatures. Gravity contours west of Winthrop (Kane and Bromery, 1966) suggest the possibility that the plutons found here may also follow the same pattern of intrusive style. The numerous small igneous bodies west of the study area (Fig. 1) may actually be cupolas of a larger granitic sheet at depth, whose eastern limit lies just west of the Augusta quadrangle. These plutons acted as sources of both heat and water, contributing to the sillimanite-grade metamorphism as well as imposing lower temperature conditions on the former andalusite–biotite terrane. This model agrees well with other studies in Maine which relate various metamorphic episodes to groups of igneous bodies as well as to individual plutons (Guidotti, 1970b, 1974; Boone, 1973; Moench and Zartman, 1976; Ferry, 1976a).

The ultimate heat source responsible for the distribution of regional isograds in Maine is unknown. In various pulses throughout the time span covering the Acadian orogeny, however, granitic magmas were generated which provided local sources of heat and water, thus forming the polymetamorphic terrane now observed in western and south-central Maine.

Acknowledgments

This paper is part of a master's thesis submitted by the senior author to Southern Methodist University. We thank Walter Anderson of the Maine Geological Survey for allowing access to aerial photographs and for use of work space during visits to the Bureau of Geology in Augusta. Thanks also go to Philip Osberg for an introduction to the stratigraphy and structure of the Augusta–Waterville–Vassalboro area.

Robert J. Tracy, Philip Osberg, and Charles Guidotti reviewed the manuscript and offered many helpful suggestions. Financial support for electron microprobe analyses was provided by a grant from the Institute for the Study of Earth and Man at Southern Methodist University. Financial assistance for field work and other research-related activities came from NSF grant EAR76-12463 to M. J. Holdaway.

References

Albee, A. L. (1968) Metamorphic zones in northern Vermont. In E-an Zen *et al.*, Eds., Studies in Appalachian Geology: Northern and Maritime, p. 239–341. Wiley-Interscience, New York.

Anderson, P.A.M., Newton, R. C., and Kleppa, O. J. (1977) The enthalpy change of the andalusite–sillimanite reaction and the Al_2SiO_5 diagram. American Journal of Science, 277, 585–593.

Bence, A. E. and Albee, A. L. (1968) Empirical correction factors for the electron microanalysis of silicates and oxides. Journal of Geology, 76, 382–403.

Boone, G. M. (1973) Metamorphic stratigraphy, petrology and structural geology of the Little Bigelow Mountain map area, western Maine. Maine Geological Survey Bulletin 24.

Burnham, C. W., Holloway, J. R., and Davis, N. F. (1969) Thermodynamic properties of water to 1000°C and 10,000 bars. Geological Society of America Special Paper 132.

Carmichael, D. M. (1970) Intersecting isograds in the Whetstone Lake area, Ontario. Journal of Petrology, 11, 147–181.

Cheney, J. T. and Guidotti, C. V. (1979) Muscovite–plagioclase equilibria in sillimanite + quartz bearing metapelites, Puzzle Mountain area, northwest Maine. American Journal of Science, 279, 411–434.

Chinner, G. A. (1973) The selective replacement of the aluminum

silicates by white mica. Contributions to Mineralogy and Petrology, 41, 83–87.

Dallmeyer, R. D. and Vanbreeman, O. (1978) $^{40}Ar/^{39}Ar$ and Rb–Sr ages in west-central Maine: their bearing on the chronology of tectono-thermal events. (abstr.) Geological Society of America Abstracts with Programs, 10, 38.

Doyle, R. G. (Ed.) 1967) Preliminary geologic map of Maine, scale 1:500,000. Maine Geological Survey.

Eugster, H. P. and Skippen, G. B. (1967) Igneous and metamorphic reactions involving gas equilibria. In P. H. Abelson, Ed., Researches in Geochemistry, II, p. 492–520. John Wiley and Sons, New York.

Ferry, J. M. (1976a) Metamorphism of calcareous sediments in the Waterville–Vassalboro area, south-central Maine. American Journal of Science, 276, 841–882.

Ferry, J. M. (1976b) P, T, $f(H_2O)$ during metamorphism of calcareous sediments in the Waterville–Vassalboro area, south-central Maine. Contributions to Mineralogy and Petrology, 57, 119–143.

Ferry, J. M. and Spear, F. S. (1978) Experimental calibration of the partitioning of Fe and Mg between biotite and garnet. Contributions to Mineralogy and Petrology, 66, 113–117.

Fisher, L. W. (1941) Structure and metamorphism of Lewiston, Maine, region. Geological Society of America Bulletin, 52, 107–160.

French, B. M. (1966) Some geological implications of equilibrium between graphite and a C–H–O gas phase at high temperatures and pressures. Reviews of Geophysics, 4, 223–253.

Green, J. C. (1963) High-level metamorphism of pelitic rocks in northern New Hampshire. American Mineralogist, 48, 991–1023.

Griffin, D. T. and Ribbe, P. H. (1973) The crystal chemistry of staurolite. American Journal of Science, 273A, 479–495.

Guidotti, C. V. (1963) Metamorphism of the pelitic schists in the Bryant Pond quadrangle, Maine. American Mineralogist, 48, 772–791.

Guidotti, C. V. (1968) Prograde muscovite pseudomorphs after staurolite in the Rangeley–Oquossoc areas, Maine. American Mineralogist, 53, 1368–1376.

Guidotti, C. V. (1970a) The mineralogy and petrology of the transition from the lower to upper sillimanite zone in the Oquossoc area, Maine. Journal of Petrology, 11, 277–336.

Guidotti, C. V. (1970b) Metamorphic petrology, mineralogy, and polymetamorphism in a portion of N.W. Maine. In G. M. Boone, Ed., 1970 New England Intercollegiate Geological Conference, 62nd Annual Meeting. Field trip B-1, 1–29.

Guidotti, C. V. (1974) Transition from staurolite to sillimanite zone, Rangeley quadrangle, Maine. Geological Society of America Bulletin, 85, 475–490.

Guidotti, C. V. and Cheney, J. T. (1976) Margarite pseudomorphs after chiastolite in the Rangeley area, Maine. American Mineralogist, 61, 431–434.

Hewitt, D. A. and Wones, D. R. (1975) Physical properties of some synthetic Fe–Mg–Al trioctahedral biotites. American Mineralogist, 60, 854–862.

Holdaway, M.J. (1971) Stability of andalusite and the aluminum silicate phase diagram. American Journal of Science, 271, 97–131.

Holdaway, M. J. (1978) Significance of chloritoid and staurolite-bearing rocks in the Picuris Range, New Mexico. Geological Society of America Bulletin, 89, 1404–1414.

Hoschek, G. (1969) The stability of staurolite and chloritoid and their significance in metamorphism of pelitic rocks. Contributions to Mineralogy and Petrology, 22, 208–232.

Huebner, J. S. (1971) Buffering techniques for hydrostatic systems at elevated pressures. In G. C. Ulmer Ed., Research Techniques for High Pressure and High Temperature, p. 123–177. Springer-Verlag, New York.

Kane, M. F. and Bromery, R. W. (1966) Simply Bouguer gravity map of Maine. U. S. Geological Survey Geophysical Investigations Map GP-580.

Kane, M. F. and Bromery, R. W. (1968) Gravity anomalies in Maine. In E-an Zen *et al.*, Eds., Studies of Appalachian Geology: Northern and Maritime, p. 415–423. Wiley-Interscience, New York.

Kane, M. F., Bromery, R. W., Simmons, G., Diment, W. H., Fitzpatrick, M. M., and Joyner, W. B. (1972) Bouguer gravity and generalized map of New England and adjoining areas. U. S. Geological Survey Geophysical Investigations Map GP-839.

Kerrick, D. M. (1974) Review of metamorphic mixed-volatile (H_2O–CO_2) equilibria. American Mineralogist, 59, 729–762.

Moench, R. H. and Zartman, R. E. (1976) Chronology and styles of multiple deformation, plutonism, and polymetamorphism in the Merrimack synclinorium of western Maine. Geological Society of America Memoir, 146, 203–238.

Newton, R. C. (1966) Kyanite–andalusite equilibrium from 700° to 800°C. Science, 153, 170–172.

Nielson, D. L., Clark, R. G., Lyons, J. B., Englund, E. J., and Borns, D. J. (1976) Gravity models and mode of emplacement of the New Hampshire Plutonic Series. Geological Society of America Memoir, 146, 301–318.

Novak, J. M. (1978) Metamorphic petrology, mineral equilibria, and polymetamorphism in the Augusta quadrangle, south-central Maine. M. S. Thesis, Southern Methodist University, Dallas, Texas.

Ohmoto, H. and Kerrick, D. M. (1977) Devolitization equilibria in graphitic systems. American Journal of Science, 277, 1013–1044.

Osberg, P. H. (1968) Stratigraphy, structural geology, and metamorphism of the Waterville–Vassalboro area, Maine. Maine Geological Survey Bulletin 20.

Osberg, P. H. (1971) An equilibrium model for Buchan-type metamorphic rocks, south-central Maine. American Mineralogist, 56, 570–586.

Osberg, P. H. (1974) Buchan-type metamorphism of the Waterville pelite, south-central Maine. In P. H. Osberg, Ed., 1974 New England Intercollegiate Geological Conference, 66th Annual Meeting. Field trip B-6, 210-222.

Osberg, P. H., Moench, R. H., and Warner, J. (1968) Stratigraphy of the Merrimack synclinorium in west-central Maine. In E-an Zen *et al.*, Eds., Studies of Applachain Geology: Northern and Maritime, p. 241–253. Wiley-Interscience, New York.

Pankiwskyj, K. A., Ludman, A., Griffen, J. R., and Berry, W. B. N. (1976) Stratigraphic relationships on the southeast limb of the Merrimack synclinorium in central and west-central Maine. Geological Society of America Memoir, 146, 263–280.

Richardson, S. W., (1968) Staurolite stability in a part of the system Fe–Al–Si–O–H. Journal of Petrology, 9, 467–488.

Richardson, S. W. Gilbert, M. C., and Bell, P. M. (1969) Experimental determination of kyanite–andalusite and andalusite–sillimanite equilibria: the aluminum silicate triple point. American Journal of Science, 267, 259–272.

Robie, R. A., Hemingway, B. S., and Fisher, J. R. (1978) Thermodynamic properties of minerals and related substances at 298.15K and 1 bar (10^5 pascals) pressure and at higher temperatures. U.S. Geological Survey Bulletin 1452.

Ryzhenko, B. N. and Volkov, V. P. (1971) Fugacity coefficients of some gases in a broad range of temperatures and pressures. Geochemistry International, 8, 468–481.

Skinner, B. J. (1956) Physical properties of end-members of the garnet group.American Mineralogist, 41, 428–436.

Thompson, A. B. (1976) Mineral reactions in pelitic rocks: II. Calculation of some *P–T–X* (Fe–Mg) phase relations. American Journal of Science, 276, 425–454.

Thompson, J. B., Jr. (1957) The graphical analysis of mineral assemblages in pelitic schists. American Mineralogist, 42, 842–858.

Tracy, R. J. (1978) High grade metamorphic reactions and partial melting in pelitic schist, west-central Massachusetts. American Journal of Science, 279, 150–178.

Tracy, R. J., Robinson, P., and Thompson, A. B. (1976) Garnet composition and zoning in the determination of temperature and pressure of metamorphism, central Massachusetts. American Mineralogist, 61, 762–775.

Vernon, R. H. and Flood, R. H. (1977) Interpretation of metamorphic assemblages containing fibrolitic sillimanite. Contributions to Mineralogy and Petrology, 59, 227–235.

Winkler, H. G. F. (1979) Petrogenesis of Metamorphic Rocks, 5th edition. Springer-Verlag, Heidelberg.

Zartman, R. E., Hurley, P. M., Krueger, H. W., and Giletti, B. J. (1970) A Permian disturbance of K–Ar radiometric ages in New England—its occurrence and cause. Geological Society of America Bulletin, 81, 3359–3374.

Zharikov, V. A., Shmulovich, K. I., and Bulatov, V. K. (1977) Experimental studies in the system $CaO–MgO–Al_2O_3–SiO_2–CO_2–H_2O$ and conditions of high temperature metamorphism. Tectonophysics, 43, 145–162.

Manuscript received, August 2, 1979;
accepted for publication, June 17, 1980.